Pattern Recognition in Real Time using Neural Networks: An Application for Pressure Measurement

Parham Piroozan
Department of Mechanical Engineering, California State Polytechnic University, 3801 W Temple Ave, Pomona, CA 91768, U.S.A.

Keywords: Real-time Recognition of Fringe Patterns, Neural Networks, Interferometric Reflection Moiré, Pressure Sensor, Electro-optic System.

Abstract: Retrieving information in real time from fringe patterns is a topic of great importance in scientific and engineering applications of optical methods. This paper describes an application of neural networks for real time pressure measurement using fringe pattern recognition. It is based on the capability of neural networks to recognize signals that are similar but not identical to the signals which were used to train the network. In this investigation a pressure sensor, which was part of the wall of the wind tunnel, and an optical apparatus were used to produce moiré fringes. The fringe patterns generated were analyzed by a back propagation neural network at the speed of the recording device, which was a CCD camera with a pixel resolution of 649 (H) x 491 (V). This method of information retrieval was used to measure the pressure fluctuations in the boundary layer flow. A second neural network was used to recognize the pressure patterns and to provide input to a control system that was capable to preserve the stability of the flow.

1 INTRODUCTION

Determination of frequency in fringe patterns is of great importance in many applications of optical methods in engineering (Sciammarella and Kim, 2005). This paper presents a technique to find fringe pattern frequencies in real-time. Real-time refers to timing within the range of frequencies of the recording devices such as CCD cameras. In this paper, an optical pressure sensor, which is capable of producing moiré fringes, is introduced. The optical pressure sensor was part of the wall of the wind tunnel and was used to instantaneously measure the pressure fluctuations in the boundary layer flow. The optical apparatus used was a reflection moiré interferometer. The Helium-Neon laser light was used to illuminate the reflecting surface of the pressure sensor, which was displaced due to wall pressure fluctuations by a few light wavelengths. A CCD camera recorded instantaneous fringe patterns. These fringes were slope fringes which were used for the pressure measurements by a back propagation neural network. The wall area observed was approximately 76 mm x 76 mm. The flow velocity outside the boundary layer was 6.2 m/sec. Wall pressure was both positive and negative and was in the order of ± 5.0 x 10^{-4} psi (Piroozan, 1997).

In the moiré interferometer developed in the present investigation, slope of the deformed membrane generated straight and vertical (constant slope) moiré fringes, which were linearly proportional to the pressure on the membrane, and were the source of information used for the wall pressure measurement.

The optical system provided 15 x 15 arrays of inputs corresponding to the 15 x 15 array of diaphragms of the pressure sensor to a back propagation neural network that analyzed the received signals and classified them into four pressure levels. The classified pressures were a 15 x 15 array of numbers ranging from 1 to 4. These numbers were then input to a second back propagation neural network which was used to recognize the pressure patterns. The output from the back propagation neural network used for pattern recognition provided real-time input to a control system for fluid flow control. Figure 1 shows a schematic representation of the main components used in the neural network reading process.

Piroozan, P.
Pattern Recognition in Real Time using Neural Networks: An Application for Pressure Measurement.
DOI: 10.5220/0005673105660572
In *Proceedings of the 5th International Conference on Pattern Recognition Applications and Methods (ICPRAM 2016)*, pages 566-572
ISBN: 978-989-758-173-1

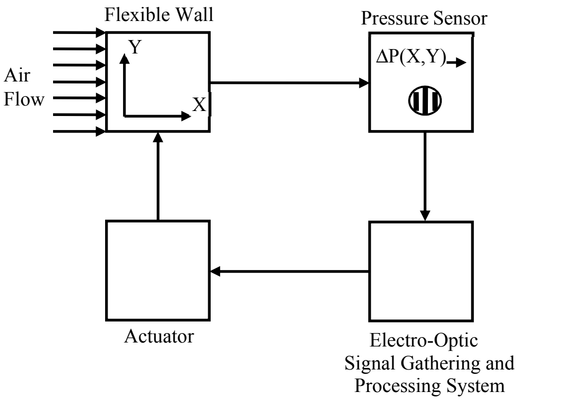

Figure 1: Schematic representation of the neural network reading process.

2 PRESSURE SENSOR

The optical pressure transducer was based on measuring the slopes of an array of diaphragms using a moiré interferometer. The diaphragms were formed by stretching an elastic membrane over an array of holes drilled on a circular disk, which was set into the boundary layer flow (Figure 2) (Piroozan, 1997).

A 15 x 15 array of holes each with a diameter of 4 mm and center-to-center distance of 5 mm were drilled through the disk. The diameter and spacing of the holes were selected to give a spatial resolution of

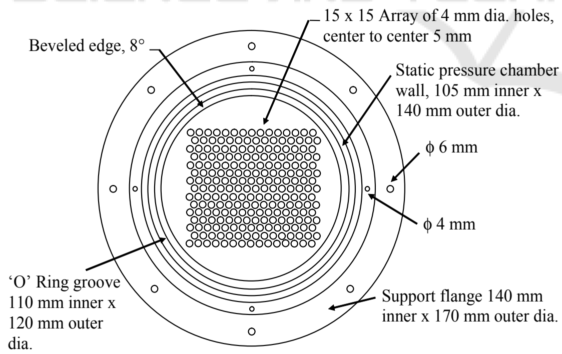

Figure 2: Pressure sensor layout.

approximately 4 holes per span-wise wavelength of the stream-wise vortex mode in the experiment. The holes were spaced evenly in the span-wise and stream-wise directions. These holes collectively made a square, 76.5 mm in width and 74 mm in height, which was illuminated by a light beam with a diameter of 105 mm.

The measuring (front) surface of the disk was covered with a thin layer of cellulose nitrate (nitrocellulose) membrane covered with a thin layer of aluminum. It formed an optical quality mirror surface, which was part of a moiré interferometer. Figure 3 shows a computer generated pressure field used for implementing the required software. This Figure shows the moiré fringe patterns for each of the 15 x 15 array of diaphragms of the pressure sensor (Figure 2) for a pressure ranging between $\pm 5.0 \times 10^{-4}$ psi.

3 OPTICAL ARRANGEMENT

Figure 4 shows the shear interferometer used for the wall pressure measurement. The optical arrangement was mounted on a steel structure beside the wind tunnel. A 10.0 milliwatt linearly polarized Helium Neon laser was used as the light source. Diameter of the laser beam was expanded from 0.95 mm to 150 mm by using: a microscope objective with a magnification of 63x and focal length of 2.94 mm, a 5 μm pinhole,

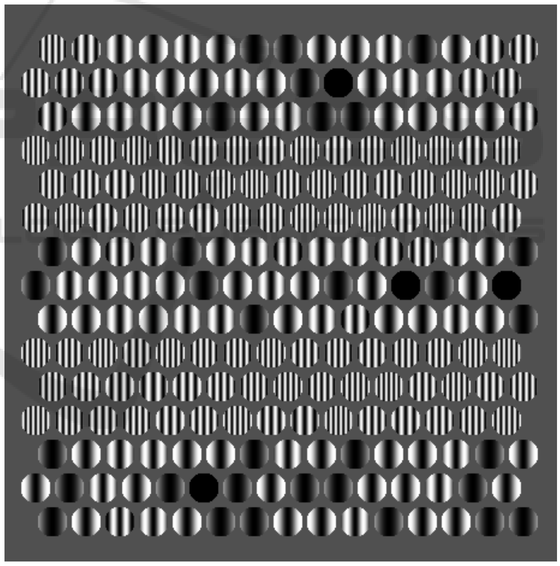

Figure 3: Simulated pressure field used to develop the software of the pressure sensing system.

and a collimating lens with a focal length of 762 mm (30 inches) and diameter of 152 mm (6 inches). Collimated light passed through a 1000 line/inch grating and was reflected by the pressure sensor after passing through a non-reflecting, optically flat glass with a diameter of 279 mm (11 inches) which was mounted on the wind tunnel wall. Reflected light then passed through the non-reflecting glass and then a telecentric system of lenses. The telecentric system of lenses consisted of two identical lenses with focal

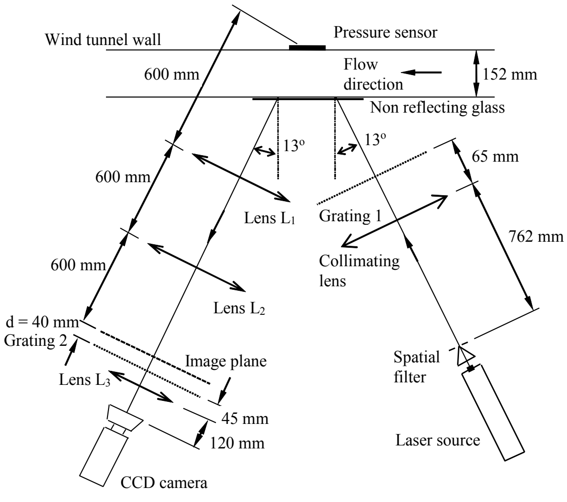

Figure 4: Optical setup used for creating moiré fringes.

lengths of 600 mm and diameters of 120 mm which reproduced the pressure sensor at the focal point of the second lens. The second grating was placed after the telecentric system of lenses and was identical with the first grating with a frequency of 1000 line/inch. This grating was placed at a distance d from the focal point of the second lens of the telecentric lens system, where the pressure sensor was reproduced. Sensitivity was increased by increasing the distance d. The third lens used had a focal length of 128.7 mm and diameter of 76 mm which was used to focus the fundamental harmonic (order +1 or -1) and order 0 into the CCD camera. This was done by slightly rotating lens L_3 about its vertical axis.

Figure 5 shows the elastic membrane stretched over a pressure sensor. Slope of the membrane is given by (Piroozan, 1997),

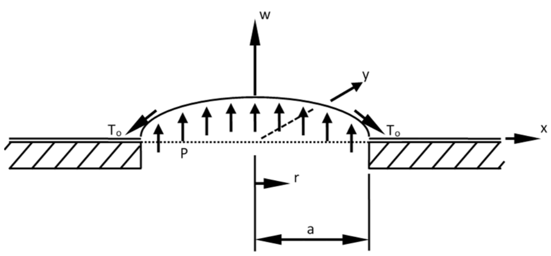

Figure 5: Elastic membrane stretched over a pressure sensor.

$$\left|\frac{\partial \mathrm{w}}{\partial r}\right| = \frac{\mathrm{Pr}}{2\mathrm{T_o}} \tag{1}$$

where P is the pressure differential over the membrane, T_o is the tension in the membrane, and r is the distance measured from the center of each sensor. Equation (1) shows that fringes are a linear function of the pressure differential over the membrane. Figure 6 shows the constant slope moiré fringes recorded using the optical setup shown in Figure 4 for a 3 x 3 version of the pressure sensor (Ligtenberg, 1955).

4 PRESSURE LEVELS MEASUREMENT: NEURAL NETWORKS

For the complete process of flow control, the sensor had to measure the pressure at the 225 points defined by the 15 x 15 array of membranes in one cycle, that is in 1/30 second (33 milliseconds). There is no time to apply methods of fringe analysis to obtain the pressure values. For this reason a back propagation neural network was selected to read the patterns and to classify the readings in real time into pressures. A back propagation network can be used for the purpose of recognizing signals similar but not totally identical to those which have been used for training the network. The architecture of the network is illustrated in Figure 7: there is an input layer, an output layer, and a hidden layer, all interconnected. The training of a feedback network requires three stages: (a) feed forward of the patterns used for the training, (b) determination of error terms at each node via the back propagation strategy, and (c) adjustment of the weights. In the recognition phase of the network only the forward part is applied, hence the

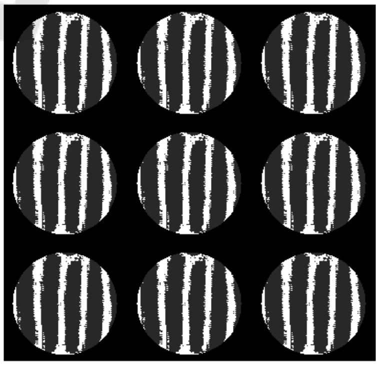

Figure 6: Constant slope moiré fringes recorded over a 3 x 3 version of the pressure sensor.

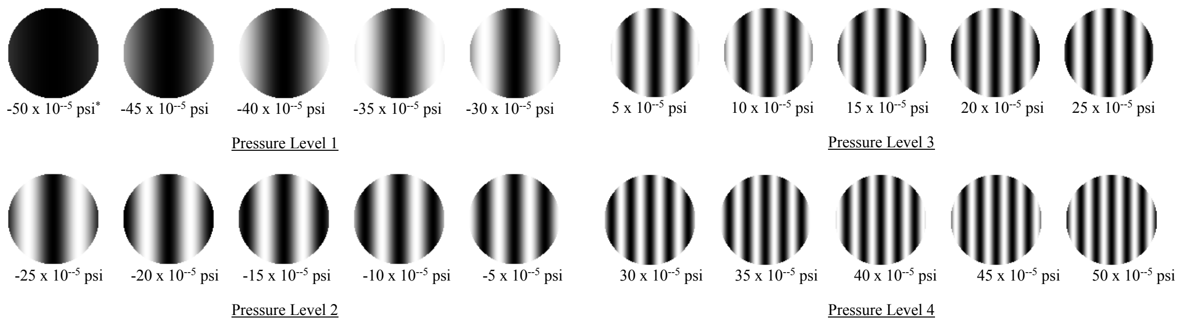

Figure 8: Simulated pressure patterns (levels 1 and 2 correspond to negative pressures, levels 3 and 4 correspond to positive pressures).

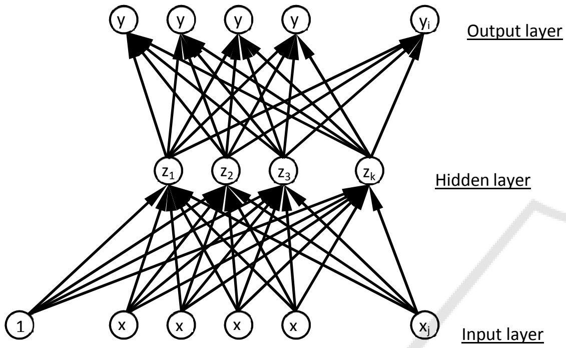

Figure 7: Schematic representation of the back propagation network utilized to classify and read fringes.

The accuracy of the obtained results depends on the training phase of the network. The same circuit will provide different results with different trainings. There are two important goals to fulfill in the design of the network:

a) All expected classes of inputs must be represented in the training process. The separation between classes must be adequately represented.
b) Within each class, all the possible variations must be present.

The size of the required training samples depends on the size of the network. There is a rule of thumb of having at least twice as many samples as the number of weights present in the network.

The input to the system is a series of calibration patterns. Two types of calibrations were performed in this particular application: static and dynamic calibrations. In the static calibration, pre-selected pressures were applied to the sensors, the images were recorded and stored in the computer memory. The dynamic pressure calibration was utilized to verify the static calibration and to see if there is any dynamic resonant effect in the patterns. The static calibration patterns were utilized as input for the neutral network. Figure 8 shows a computer-generated set of calibration pressures used in the preliminary developments of the system. In this preliminary work, the whole process was digitally simulated. The levels of pressure were subdivided into four levels with the limits indicated in Figure 8.To analyze the pressure distribution in a given region, an array containing a number of equally spaced sensors is utilized. Each sensor gives the average pressure in a region (area of the sensor). This area is selected by considerations involving the physical size of the structures in the flow that one wants to detect, the sensibility of the individual sensors, the CCD camera sensor size, the number of pixels, and the optical system.

Figure 3 showed a computer-generated pressure field used for implementing the required software. Figure 9 shows the output matrix corresponding to the patterns of Figure 3. The neural networks software used to carry out this operation was NeuralWorks Professional II/Plus (NeuralWare Inc.).

For purposes of comparing experimental (hot wire) measurements and numerical computation values, pressure measurements were done for a 1 x 7 array of the pressure sensor. 1,050 fringe patterns

4	2	2	1	2	1	1	1	1	1	2	1	1	2	2
3	2	2	2	1	1	2	1	1	1	1	2	2	2	2
2	1	2	2	1	1	1	2	1	1	1	1	2	1	2
4	4	4	4	4	3	4	3	4	3	4	4	4	3	4
4	3	3	4	4	4	4	4	4	4	3	4	4	4	3
4	4	3	4	3	3	4	4	4	4	4	3	4	4	3
1	1	2	2	1	1	2	2	2	2	2	2	2	1	1
1	2	1	2	1	1	1	2	1	1	1	1	1	1	1
1	1	2	1	2	2	1	1	2	2	1	1	2	1	1
4	4	4	3	4	4	4	4	3	4	3	4	4	4	4
4	3	3	2	3	3	4	4	4	4	4	3	4	3	4
4	4	3	4	3	3	4	3	2	4	3	3	3	4	4
1	1	2	2	1	1	1	2	1	1	1	1	2	1	1
1	1	2	1	1	1	1	1	1	1	1	1	2	1	1
1	1	2	2	1	1	1	1	1	2	1	1	1	1	1

Figure 9: Output of the neural network corresponding to the pressure field shown in Figure 3.

from the array with known pressures in the range of ±0.0005 psi were recorded. Each record consisted of 24 positive integers ranging from zero to 255 which were the minimum and maximum pixel values in an eight-bit frame. These numbers were input to a back propagation neural network with 24 processing elements in the input layer. Figure 10 shows the input to the back propagation neural network from each individual sensor.

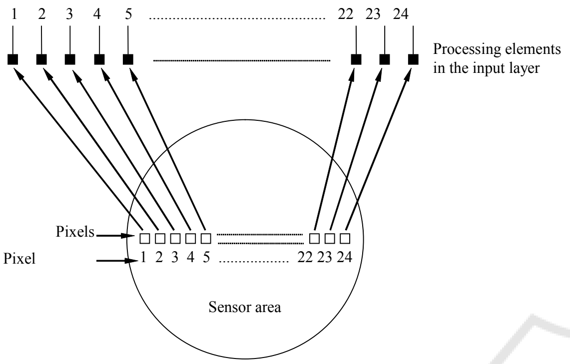

Figure 10: Input data from a sensor to the input layer of the back propagation neural network for pressure classification.

Number of samples were doubled by writing the input vector in normal $\{a_1, a_2, a_3, \dots, a_{24}\}$ as well as in reverse order $\{a_{24}, a_{23}, a_{22}, \dots, a_1\}$, where a represents the pixel value. By doing so, not only the number of samples was increased, but also phase differences arising from the different sensors and possible noise were also included. These patterns were used to train and test the back propagation neural network. 1,750 of the records (out of the total of 2,100) were used for training while the remaining 350 records were used to test the performance of the network. The network consisted of an input layer, one output layer, and one hidden layer as shown in Figure 11.

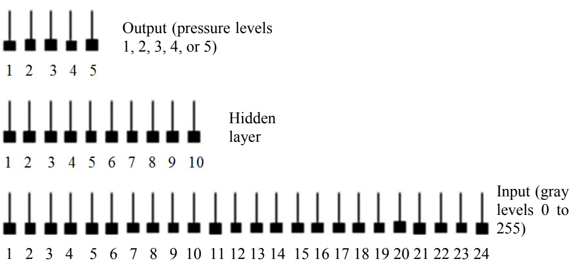

Figure 11: The back propagation neural network used for the pressure classification.

There were 24 processing elements in the input layer, ten processing elements in the hidden layer, and five processing elements in the output layer which were fully interconnected (connections are not shown in Figure 11). The input consisted of positive integers ranging from zero to 255. The input data was first mapped to lie between +1 and -1 (bipolar format) by selecting the “Bipolar Inputs” and “MinMax Table”

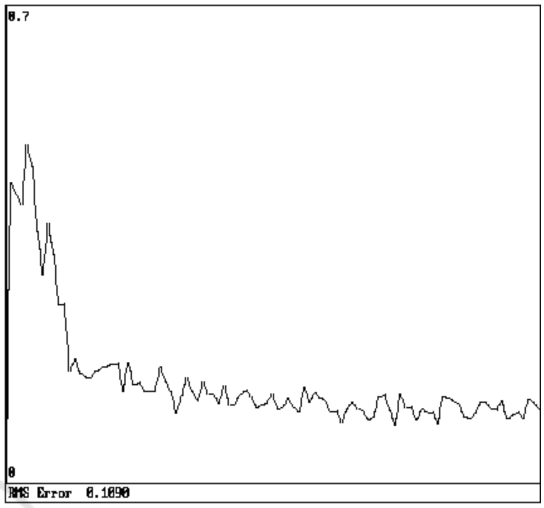

Figure 12: RMS error of the back propagation network used for pressure classification.

options from the neural networks software (NeuralWare, 1993). The “SoftMax Output” option was also used to force the components of the desired output to add up to one (one of n code). The tangent hyperbolic function was used as the activation function while normalized cumulative delta rule was used as the learning rule. Compared to other activation functions such as sine or sigmoid functions, tangent hyperbolic gave better results. Epoch was also set to 350, which was approximately the number of training records in each pressure level. By doing so, weights were updated after 350 learning cycles. This resulted in a better performance by the network as compared to selecting 1750 (total number of training records) or using the default setting value of 16. Figure 12 shows the Root Mean Square (RMS) error during the training session (RMS error is a common measure of the performance of a network). The RMS error adds up the squares of the errors for each processing element in the output layer, divides by the number of processing elements in the output layer to obtain an average value, and then takes the square root of that average value. The network ceased to learn after the RMS error converged to approximately 0.10. This may be in part due to inaccuracies in the input data used for training the network. Inaccuracies are mainly due to the pressure fluctuations in the air in the lab which is of the same order of magnitude as the pressures set for calibration.

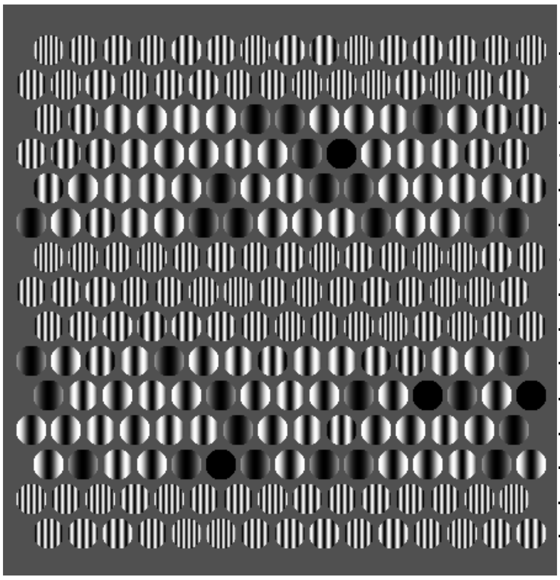

4	4	3	4	3	3	4	3	2	4	3	3	3	4	4	1
4	4	3	4	3	3	4	4	4	4	4	3	4	4	3	1
4	2	2	1	2	1	1	1	1	1	2	1	1	2	2	0
3	2	2	2	1	1	2	1	1	1	1	2	2	2	2	0
2	1	2	2	1	1	1	2	1	1	1	1	2	1	2	0
1	1	2	2	1	1	1	1	1	2	1	1	1	1	1	0
4	4	4	4	4	3	4	3	4	3	4	4	4	3	4	1
4	3	3	4	4	4	4	4	4	4	3	4	4	4	3	1
4	3	3	2	3	3	4	4	4	4	4	3	4	3	4	1
1	1	2	2	1	1	2	2	2	2	2	2	2	1	1	0
1	2	1	2	1	1	1	2	1	1	1	1	1	1	1	0
1	1	2	1	2	2	1	1	2	2	1	1	2	1	1	0
1	1	2	1	1	1	1	1	1	1	1	1	2	1	1	0
4	4	4	3	4	4	4	4	3	4	3	4	4	4	4	1
4	3	3	4	4	4	4	3	3	4	3	4	4	3	3	1

(a) (b) (c)

Figure 14: (a) Computer generated pressure field, and the (b) corresponding classified pressure field output from neural networks. (c) output signals from pattern recognition neural networks.

Figure 12 shows that the RMS error has converged during the learning session, which means that input patterns are learned by the network in spite of the inaccuracies in the input data. In testing, the trained network gave 56 mistakes out of the 350 records used for testing (testing was done by pressure patterns with known pressure levels), that is, 84% correct answers. The source code generated from the trained network was then used for the real pressure classification.

To make the operation fast, data from only one row of each pressure sensor was used for the pressure measurement. Each row was represented by 24 pixels per sensor. Images were frozen during the data acquisition process. Analysis was done sequentially for each sensor. The output was a 1 x 7 array consisting of integers 1 through 5 corresponding to the five pressure levels.

5 PROCESS TO ANALYZE THE PRESSURE PATTERNS

The pressure pattern is characterized by elongated features, vortices, in the direction of the flow. In the transversal direction these features are of the order of three sensor spacing wide. Through theoretical and experimental results the shape of the features is known and only actual dimensions (width and position of the longitudinal vortices) are not known. Figure 13 shows the expected pressure field.

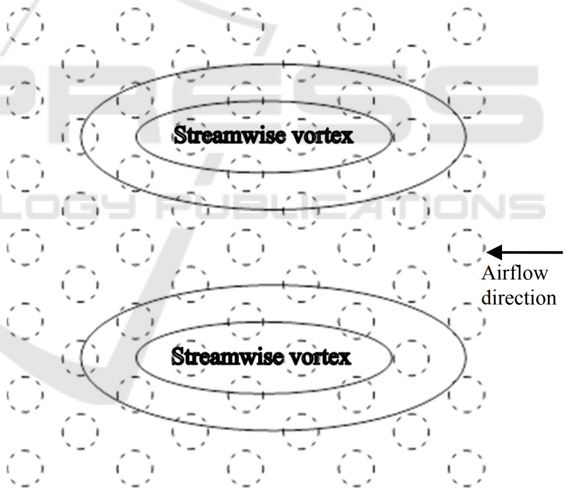

Figure 13: The expected pressure field.

The complete process of pressure measurement and pattern recognition was done by using computer generated and expected pressure fields for the 15 x 15 array of sensors. Figure 14 shows a sample of the computer generated pressure field with the corresponding output from the back propagation neural networks for pressure classification and pattern recognition. Pressures were classified into four levels. The back propagation neural network used for pressure pattern recognition consisted of an input layer with 225 processing elements, a hidden layer with 50 processing elements and an output layer with 15 processing elements. The training patterns with the desired output vectors were used to train the back propagation neural network. "Delta-Rule" and "Sigmoid" function were used as the learning rule and the activation function. "Bipolar Inputs" was deselected and Epoch was selected as 16. After about 5,000,000 iterations, the training set converged and the network was tested with the patterns that the network had not seen before (these patterns were not used for training the network). The 15 outputs from the network were exactly the same as the desired output vectors as shown in Figure 14 (c).

6 CONCLUSIONS

From the obtained patterns it can be concluded that the back-propagation neural network used for pattern classification and pressure measurement proved to work satisfactorily especially for noisy inputs.

Pressure fluctuations in the boundary layer were extremely small in the order of $\pm 5.0 \times 10^{-4}$ psi. When dealing with small pressures, calibration (gathering the training and testing data) proved to be a problem due to very small random fluctuations in the atmospheric pressure in the laboratory due to external causes (wind blowing, opening or closing doors in neighboring rooms). Calibration and data gathering must be done with static pressures applied to the pressure sensor with no pressure fluctuations present in the surrounding air.

Successful operation of the pressure classification and pattern recognition to a large extend depends on the quality of the fringe patterns and the signals generated by the electro-optical system, in particular, the pressure sensor. Great care must be taken in the selection and fabrication of the membrane material.

The computer code used for the pattern recognition of the 15 x 15 array consists of approximately 6000 lines of C programming. Operating systems such as Windows or DOS and C compilers running on these platforms are not adequate, or, can handle this job very slowly. It is recommended to operate the image processing system and the neural networks on work stations with UNIX operating system.

Determination of fringe pattern frequencies in real time has a variety of interesting applications in the future as viewed from the recent developments (Sciammarella and Kim, 2005). Neural networks proved to be a powerful tool which can be utilized for this purpose.

ACKNOWLEDGEMENTS

The research work presented in this paper was done in collaboration with Dr. Cesar A. Sciammarella, Professor of the Department of Mechanical, Materials, and Aerospace Engineering, Illinois Institute of Technology, USA, and Dr. Thomas Corke, Clark Chair Professor of the Department of Mechanical and Aerospace Engineering, Notre Dame University, USA. To them goes my deep appreciation and recognition for their innumerable contributions to the project.

REFERENCES

Sciammarella, C.A., Kim, T., 2005. Frequency modulation interpretation of fringes and computation of strains. In *Experiemntal Mechanics 2005;45:393-403.*

Sciammarella, C. A., Piroozan, P., 2007. Real-time determination of fringe pattern frequencies: An application to pressure measurement. In *Optics and Lasers in Engineering 45 (2007) 565-577.*

Piroozan, P., 1997. Pressure sensor to determine spatial pressure distribution in boundary layer flows. *Ph.D., Illinois Institute of Technology.*

Emmerling, R., 1973. The instantaneous structure of the wall pressure under a turbulent boundary layer flow. *Max-Planck-Institut Fur Stromungsforschung, Gottingen, Bericht Nr. 9.*

Dinkelacker, A., Hessel, M., Meier, G. E. A., Schewe, G., 1977. Investigation of pressure fluctuations beneath a turbulent boundary layer by means of an optical method. In *The Physics of Fluids, Vol. 20, No. 10, Pt. 11.*

Ligtenberg, F. K., 1955. The moiré method and new experimental method in the determination of moments in small slab models. In *Proceedings of the Society of Experimental Stress Analysis, V, XII, No. 2, pp. 82-98.*

Fausett, L., 1994. *Fundamentals of Neural Networks: Architectures, Algorithms, and Applications*. Prentice Hall, Englewood Cliffs, New Jersey.

Freeman, J. A., Skapura, D. M., 1992. *Neural Networks: Algorithms, Applications, and Programming Techniques.* Addison-Wesley Publishing Company, Inc. Massachusetts.

Masters, T., 1993. *Practical Neural Network Recipes in C++*. Academic Press, Inc. San Diego, CA.

Masters, T., 1994. *Signal and Image Processing with Neural Networks: A C++ Sourcebook*. John Wiley & Sons, Inc. New York.

NeuralWare, 1993. *Neural Computing, A Technology Handbook for Professional II / Plus and NeuralWorks Explorer*. NeuralWare, Inc. Technical Publications Group. Pittsburgh, PA.